Spatial Copula Modeling to Examine the Effect of Extreme Winter Weather on Property Risk in the Great Lakes Region

Alonzo Finch
Department of Statistics, The George Washington University

December 19, 2025

Abstract

Recent climate research suggests that Arctic warming may be linked to increasingly severe winter weather in mid-latitudes, yet the implications for property risk remain understudied. This paper examines the relationship between extreme winter weather and relative property risk in the U.S. Great Lakes region (Illinois, Indiana, Michigan, Ohio, and Wisconsin). Because asset-level loss data are not publicly available, a composite property risk index is constructed using housing characteristics, socio-demographic variables, and physical environmental factors derived from census and geospatial data. Winter weather conditions—precipitation, snow-water equivalent, and minimum and maximum temperatures—are modeled as functional predictors using smoothed daily curves. A scalar-on-function regression framework is combined with a spatial copula model to account for spatial dependence across census tracts, estimated via latent Gaussian modeling and INLA. Results indicate that winter weather variables are statistically significant predictors of relative property risk, though they explain a modest proportion of overall variance. Incorporating seasonal lag effects improves model performance, highlighting the importance of temporal dependence. The findings suggest that functional spatio-temporal models offer a promising framework for assessing evolving winter weather risks under climate change.

Keywords: Composite Index, Spatial Functional Data Analysis, INLA

1 Introduction

1.1 Extreme Winter Weather

Over the past two decades, much of the focus of climate change research and policy activism has been focused on how temperatures have trended upward in many parts of the globe, with a particular focus on longer, more persistent summers and an increase in the frequency and magnitude of tropical storms or droughts. However, a corollary effect that has received less attention is the effect of climate change on winter weather. Cohen et al. (2014) and Kug et al. (2015) discuss how persistent arctic warming has lead to an increase in extremely harsh winters in the mid-latitudes, particularly over Asia and North America, and Williams et al. (2025) furthers this trend by showing recent evidence of a similar effect in Northern Europe.

1.2 Winter Weather and Monetary Loss

Just as with more severe tropical storms leading to more frequent flooding, and intense droughts leading to crop loss and rising prices of utilities, more frequent and more severe winter storms are also associated with an increase in the frequency of adverse events. Early work linking extreme winters storms was done in Changnon et al. (2001) and Changnon (2007), performing an initial analysis linking winter weather to monetary losses in the United States, while from the same period Klawa & Ulbrich (2003) and Schwierz et al. (2010) conducted a similar analysis in Europe. More recent studies have focused primarily on windstorms in Europe (Welker et al. 2021, Severino et al. 2023, Cusack 2023, Cerda et al. 2024, Ederen et al. 2024), with the last study specifically examining property losses being Shimkus et al. (2017) which focused on the winter storms in the New York tri-state area (commonly called Nor'easters).

Understanding the relationship of winter weather and the risk of monetary damage is important for the insurance and reinsurance industries in order to keep pace with the evolving risks driven by a rapidly changing climate. Furthermore, understanding how winter weather effects scope-specific risk, for example injury versus property, can ensure business balance their overall risk portfolio and maintain solvency over time.

1.3 Overview of Paper

This paper hopes to build upon previous analyses by examining the effect of winter weather on property risk in the Great Lakes Region (Illinois, Indiana, Michigan, Ohio, Wisconsin) using a composite index representing relative property risk. Where this paper differs from previous analyses is the use of a more modern, advanced methodology through the use of functional spatial regression with a spatial dependence modeled using a spatial copula model.

The remainder of the paper is structured as follows. Section 2 contains a description of the composite index, the functional regression model, and the spatial copula model. Section 3 includes the results of the our analysis using two different formulations of our composite index, as well as a brief discussion on model performance. An extended discussion of the model and its suitability is presented in 4. Section 5 concludes with final remarks.

2 Methods

In this section I present the composite risk index, its theoretical foundation, and the data sources used. I then describe the mathematical formulation of our functional spatial copula model, present the specifics of the functional layer of the model, and introduce the spatial dependence handling using the spatial copula layer. I also include a comparison to methods used in previous analyses.

2.1 Composite Risk Index

Actual asset-level property loss and claim data is extremely difficult to access for researchers. Previous studies have relied on publicly reported monetary damages, like Changnon et al. (2001), Shimkus et al. (2017), and others. The issue with such datasets is that there is often the issue of data quality, spatial resolution, and reporting frequency. For those that use higher quality loss data (Ederen et al. 2024, Cerda et al. 2024), they are often provided by insurance companies directly, or have access restricted to researchers who pay a subscription for data aggregated by multiple insurance companies at the resolution of administrative units (i.e. states, territories, etc.) (Cusack 2023, Moemken et al. 2024), however many of those sources have better data quality outside of the United States.

In lieu of more proprietary data sources, I proceeded similarly to Severino et al. (2023) and used a proxy for property risk as my outcome measure. However, instead of using a proxy that purely describes exposure, I aggregated several sources of data together to attempt to better model underlying risk.

2.1.1 Data Sources

Using data from the American Community Survey (ACS) (Bureau n.d.) and the United States Geological Survey (USGS), I developed a composite risk index as a proxy for property risk that attempts to accurately model underlying risk using components that should influence observed losses. The components of this composite risk index can be broaden divided into three categories: housing characteristics, socio-demographic characteristics, and physical environment characteristics. The ACS data are 5-year estimates at the aggregation level of census tracts, due the stability and accuracy of the estimates and the fact that census tracts are the smallest aggregation level with the best data quality. The physical environment data from USGS are from the annual National Land Cover Database releases,

and are available as downloadable rasters.

The housing characteristics used were percentage of houses built before 1960, percentage of houses using electric heating, percentage of houses occupied by the owner, number of vehicles per household, and the density of units. The socio-demographic factors used were the percentage of households with no health insurance and the percentage of households with an occupant over the age of 65. The physical environment characteristics used were land cover type as estimated from the number of pixels overlapping each spatial aggregation unit from the provided land cover rasters, as well as percentage of impervious ground. Figure 1 shows choropleth plots of a selection of variables used to develop the composite risk index. All index components were scaled using the mean and standard deviation of the component, a step that is considered best practice (Nardo et al. 2005).

2.1.2 Weighting

I took two approaches to weighting the components of my composite index: manual weighting and principal component analysis (PCA). Many government and non-government organizations use similar schemes for weighting their composite indices. Further, using PCA weights is supported by Nardo et al. (2005), Mazziotta & Pareto (2013), and others (Mazziotta & Pareto 2016, Greco et al. 2019). The formulation of the index can be shown below in Equation 1, where $R(s)$ represents the composite risk index and α_i represents the weight of the ith component. All weights were normalized to sum to 1.

$$R(s) = \sum_i \alpha_i X_i \,; \qquad \sum_i \alpha_i = 1 \tag{1}$$

For manual weighting, I used my previous research and experience to weight components such as older housing stock (percentage of pre-1960s housing) and lack of other insurance (percentage without health insurance) higher than other components that I believed to have

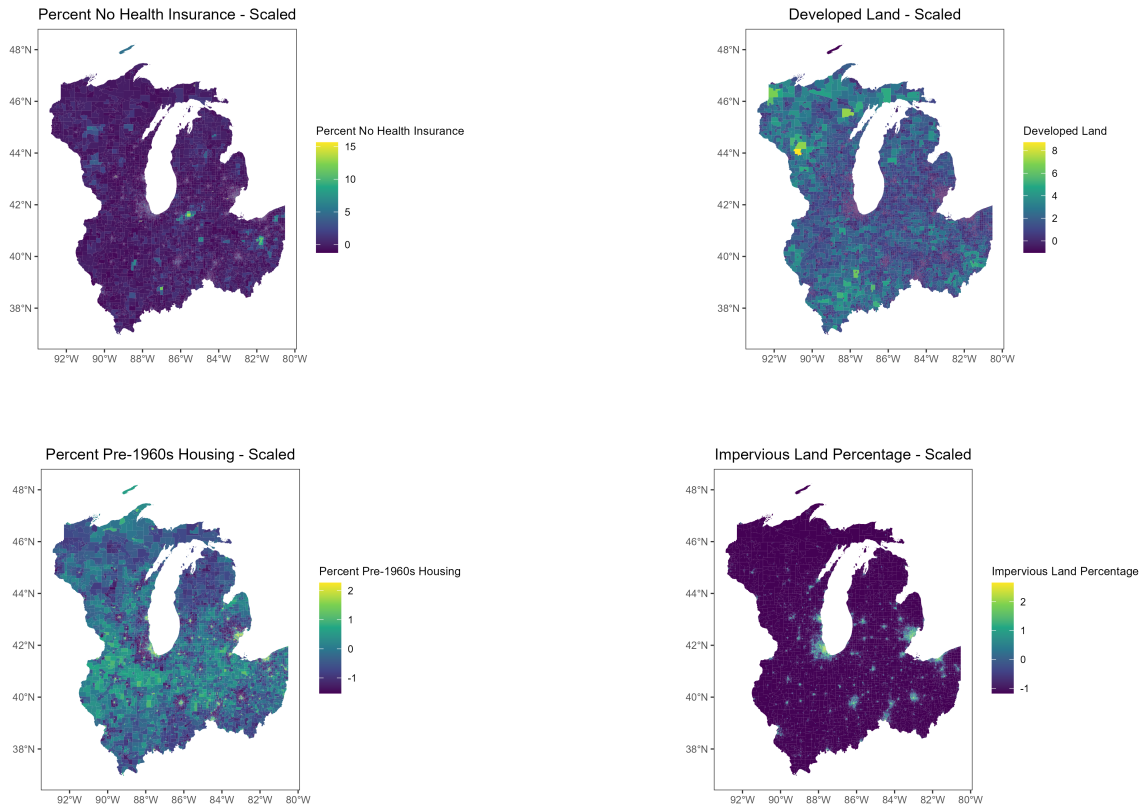

Figure 1: Choropleth plots of component variables of the composite risk index. All variables are centered and scaled, with higher values assumed to contribute more to property risk

a weaker effect on underlying risk, such as older residents (percentage 65 and over). The PCA weights were determined by aggregating the loadings and assigning those aggregated loadings as weights. The screeplot for the PCA is shown in Figure 2. The first 7 principal components were taken, as they collectively explain $\sim 75\%$ of the variance in the components (see Table 1).

2.2 Functional Model Layer

2.2.1 Data and Data Sources

Our winter weather data was obtained from Daymet Earth Science Data Systems (2025). This dataset includes daily estimates of precipitation, snow-water equivalent (swe), minimum

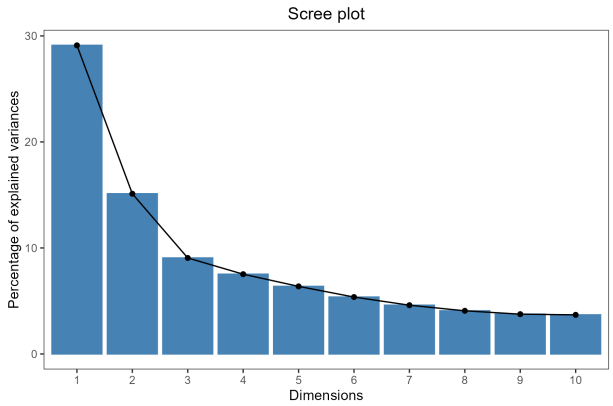

Figure 2: Screeplot for composite index PCA

Table 1: PCA Summary – Explained Variance

Truncated at principal component 7

	PC1	PC2	PC3	PC4	PC5	PC6	PC7
Standard deviation	2.224663	1.60286	1.24084	1.13104	1.041105	0.9552955	0.8843245
Proportion of Variance	0.291120	0.15113	0.09057	0.07525	0.063760	0.0536800	0.0460000
Cumulative Proportion	0.291120	0.44225	0.53282	0.60807	0.671830	0.7255100	0.7715100

temperature, and maximum temperature. Daily curves were downloaded for a period of six years (2019-2024). The curves were aggregated to the census tract level before extracting the data for the six month period of October to March. The result was 5 curves per census tract over a 6 month period capturing the winter season with a buffer on each end. The daily curves were then smoothed using a fourier basis with a roughness penalty determined through cross-validation. Figure 3 shows the resulting smoothed curves for the winter 2019 season for each of the four predictors.

2.2.2 Functional Model

The functional model is a traditional scalar-on-function regression model presented in Equation 2. Our predictors are precipitation, swe, maximum temperature, and minimum

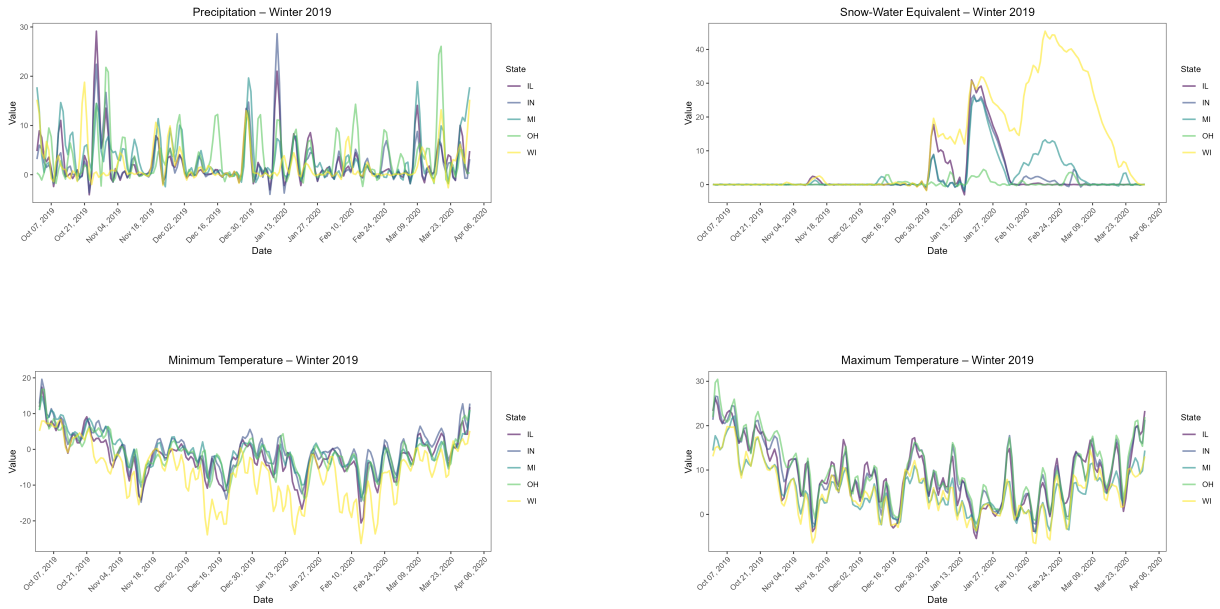

Figure 3: Fourier smoothed curves of daily curves for the winter 2019 season for a selection of census tracts. One tract is chosen from each state.

temperature, with the outcome $R(s)$ being our composite risk index scaled to the interval $[0, 1]$ to represent a relative risk. We can use the Karhunen–Loève expansion to represent our function predictors, which is shown in Equation 3, to get a computational tractable representation of our model. We selected the first 4 components ($L = 4$) to guarantee a total variance explained of at least 80%.

$$R(s) \sim \beta_0 + \int_{\tau} \mathbf{X}(t, s)\beta(t)dt + \epsilon(s) \tag{2}$$

$$R(s) \sim \beta_0 + \sum_{l=1}^{L} b_l \xi_{l,s} + \epsilon(s) \tag{3}$$

2.3 Spatial Copula Model Layer

Previous studies utilizing similar functional spatial analysis models have focused on max-stable process models Wadsworth & Tawn (2012), Bacro & Gaetan (2012), Segers (2012),

Ribatet (2013), Koch (2017). Max-stable process models rely on the assumption that our data converges asymptotically to a limiting distribution, however this is a very restrictive assumption and such a limiting distribution is not always guaranteed. That is why recent work has been moving away from max-stable processes, such Huser et al. (2024) in an aptly named paper.

I used a spatial copula to model the spatial dependence structure of the functional model presented in Section 2.2.2. We can define our model using the equation below. Our covariance matrix Σ_θ is given by the the neighborhood graph of our spatial aggreagation level. For this analysis, I chose census tracts for consistency with how data from the American Community Survey is presented since census tracts are the smallest aggregation level present for all population data. We represented our spatial dependence as a latent gaussian model so we can estimate our spatial copula using Integrated Nested Laplace Approximation (INLA), very similar to Simpson et al. (2023) and Vandeskog et al. (2024).

$$
\begin{aligned}
R(s) &\sim \beta_0 + \sum_{l=1}^{L} b_l \xi_{l,s} + \epsilon(s) \\
U(s) &= F_\epsilon(\epsilon(s)) \\
U(s_i) &\sim \text{spatial copula } C_\theta(\Sigma_\theta(i,j))
\end{aligned}
$$

3 Results

3.1 Functional Model Results

Table 2: Model Estimates - PCA Weighted Composite Index

term	edf	ref.df	statistic	p.value
s(prcp_PC1)	6.948573	7.314837	15.8196521	0.0000000
s(prcp_PC2)	7.220921	7.646554	21.3322018	0.0000000
s(prcp_PC3)	6.511027	6.978769	19.8541070	0.0000000
s(swe_PC1)	5.348085	6.013422	12.4557694	0.0000000
s(swe_PC2)	3.010509	3.690958	5.2943351	0.0006066
s(swe_PC3)	3.015278	3.692261	4.4089108	0.0027568
s(tmin_PC1)	7.718658	8.179079	27.4722501	0.0000000
s(tmin_PC2)	6.305529	6.849188	17.4126350	0.0000000
s(tmin_PC3)	6.620092	7.060132	46.4848946	0.0000000
s(tmax_PC1)	6.758642	7.218672	70.6784879	0.0000000
s(tmax_PC2)	6.044181	6.658692	27.3590366	0.0000000
s(tmax_PC3)	4.836036	5.583562	5.2602614	0.0000295
s(year)	0.000003	1.000000	0.0001396	0.0000000

Table 3: Model Estimates - Manually Weighted Composite Index

term	edf	ref.df	statistic	p.value
s(prcp_PC1)	6.7957163	7.183362	16.1203637	0.0000000
s(prcp_PC2)	7.3624104	7.792445	20.8018500	0.0000000
s(prcp_PC3)	6.5836588	7.019147	26.1195871	0.0000000
s(swe_PC1)	3.7720355	4.528719	2.7247754	0.0220233
s(swe_PC2)	2.3282716	2.922889	2.3930375	0.0645948
s(swe_PC3)	2.4653817	3.080728	15.3750075	0.0000000
s(tmin_PC1)	6.4676566	7.043274	30.4778811	0.0000000
s(tmin_PC2)	4.3620991	5.135778	25.0917926	0.0000000
s(tmin_PC3)	6.4222525	6.943159	48.9754323	0.0000000
s(tmax_PC1)	7.0973013	7.548989	108.7491972	0.0000000
s(tmax_PC2)	6.3913643	6.884749	23.5872442	0.0000000
s(tmax_PC3)	4.4450475	5.190223	6.3249892	0.0000040
s(year)	0.0000031	1.000000	0.0000954	0.0000000

Tables 2 and 3 show the estimates of our predictors for the PCA weighted composite risk index and manually weighted composite risk index respectively. We can see there is not much difference in the estimates themselves. In Tables 4 and 5 we can see the model evaluation metrics, which show us that our predictors are better estimates of the manually weighted composite risk index, however both models show an $R^2 \approx 0.07$. Overall we can say that our functional predictors only explain about 7% of the variance in either composite risk index. However, in both models, all of our terms are shown to be significant.

Table 4: Model Metrics - PCA Weighted Composite Index

df	logLik	AIC	BIC	deviance	df.residual	nobs	adj.r.squared	npar
71.33753	-8774.433	17706.15	18417.36	4848.111	62473.66	62545	0.068815	110

Table 5: Model Metrics - Manually Weighted Composite Index

df	logLik	AIC	BIC	deviance	df.residual	nobs	adj.r.squared	npar
65.4932	-8577.656	17299.28	17950.27	4817.701	62479.51	62545	0.0747425	110

3.2 Spatial Copula Model Results

To evaluate the performance of our spatial copula, we can look at Figure 4. Specifically, if we look at the PIT histograms, we see that the manually weighted composite risk index appears more uniform than that of the histogram from the PCA weighted composite risk index. This suggests that our proposed copula model is better suited to capturing the spatial dependence of the model utilizing the manually weighted composite risk index as an outcome.

Figure 4 also includes plots of Moran's I by Year. We can see sharp changes in our estimated Moran's I for each year we are evaluating. This suggests that our spatial dependence has a temporal component, and that the temporal transitions in our spatial dependence are not entirely smooth. We also see persistently high values of Moran's I, suggesting that our spatial copula model is not capturing enough of the spatial dependence.

3.3 Extension: Seasonal Lag Model

In addition to a traditional functional regression model, I examined an additional model implementing a lag term, using the information of the curves from the previous season.

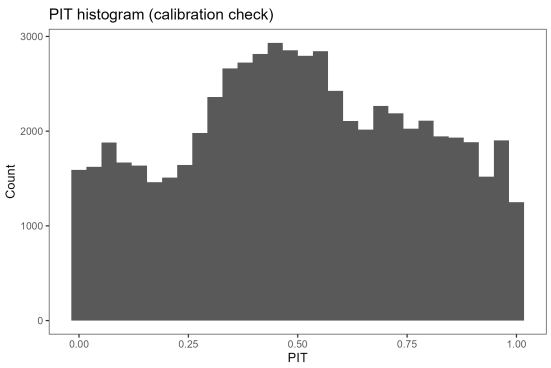

(a) PIT Histogram

PCA Weighted Index

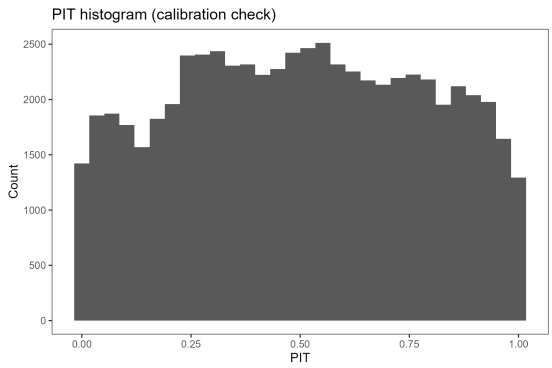

(b) PIT Histogram

Manually Weighted Index

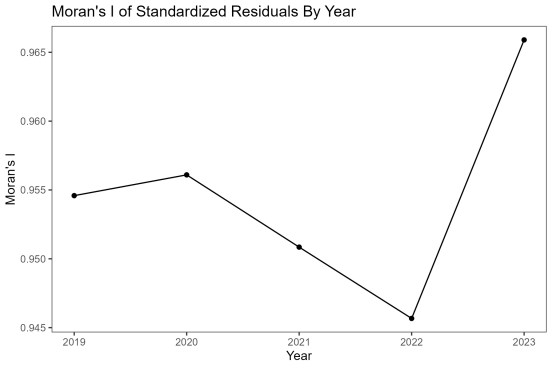

(c) Moran's I by Year

PCA Weighted Index

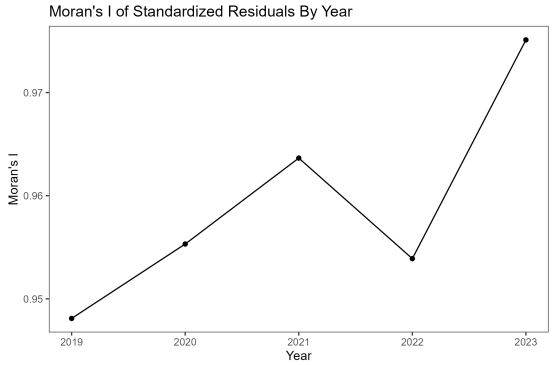

(d) Moran's I by Year

Manually Weighted Index

Figure 4: Diagnostic and evaluation plots of the spatial copula model.

Tables 6 and 7 tell a similar story to the non-lag model. The amount of variance explained by both models is relatively similar, however the addition of the lag term does improve the models to an $R^2 \approx 0.09$. We also see that by our model comparison metrics (Log-Likelihood, AIC, BIC) that our seasonal lag model is the better choice when compared to our non-lag model, despite the increased number of predictors. The estimates of both seasonal lag models are contained in the Appendix (6.1)

Examining the performance of the spatial copula layer of these models (Figure 5), we see that they are very similar across evaluation plots. We also continue to see the temporal

Table 6: Model Metrics - PCA Weighted Composite Index

Seasonal Lag Model

df	logLik	AIC	BIC	deviance	df.residual	nobs	adj.r.squared	npar
142.4979	-6365.564	13040.41	14404.42	3778.417	49893.5	50036	0.0912916	221

Table 7: Model Metrics - Manually Weighted Composite Index

Seasonal Lag Model

df	logLik	AIC	BIC	deviance	df.residual	nobs	adj.r.squared	npar
132.9416	-6276.661	12850.67	14162.04	3765.014	49903.06	50036	0.0946884	221

trend and consistently elevated value of the estimated Moran's I.

4 Discussion

Overall, our results suggest there can be significant improvement in our model. The improvement of our model with the addition of the seasonal lag terms indicates a potential area of improvement, shifting from a more traditional function regression model to potentially something like a functional Conditional Auto-Regressive (fCAR) model to model the dependence structure between seasons.

Our results also suggest that we need to improve our spatial copula model. The PIT histograms suggests potential improvement in the specification of our model, due to the fourth moment being far from uniform. We could also implement handling of temporal dependence in our spatial dependence structure. Other types of copula model estimation, such as vine copulas, could also improve our spatial copula model, and as such are a potential avenue of further research.

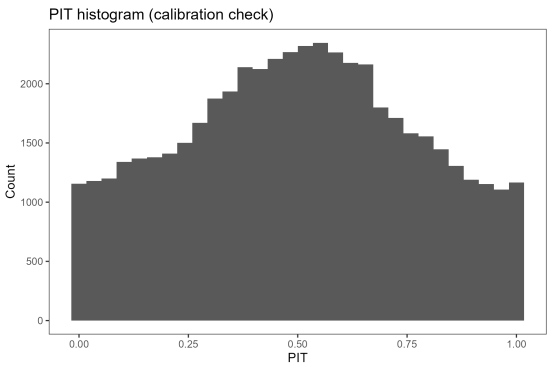

(a) PIT Histogram

PCA Weighted Index

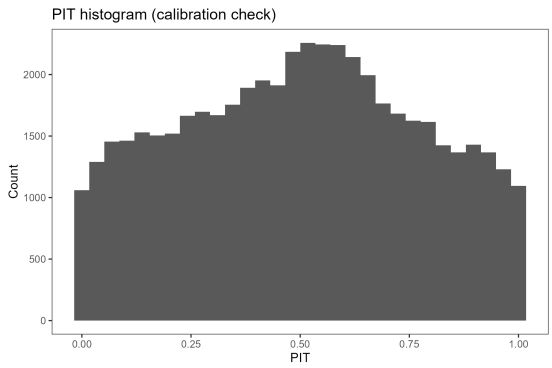

(b) PIT Histogram

Manually Weighted Index

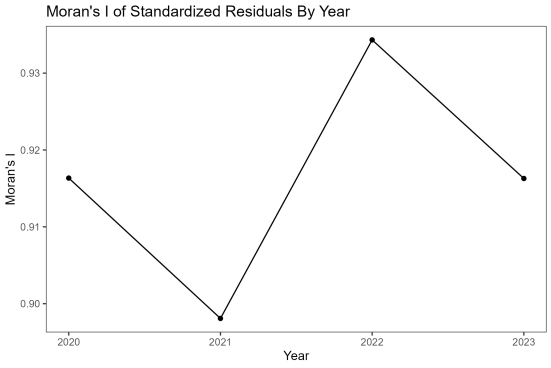

(c) Moran's I by Year

PCA Weighted Index

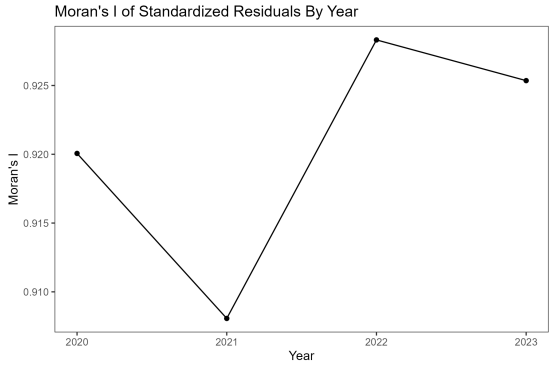

(d) Moran's I by Year

Manually Weighted Index

Figure 5: Diagnostic and evaluation plots of the spatial copula model. Based on residuals from the seasonal lag model.

Taken together, this is a clear indication that our model may significantly improve if we utilize a fully functional spatio-temporal model, instead of trying to model the spatial and temporal components separately.

4.1 Composite Risk Index

The greatest point of weakness in this study is the formulation of the composite risk index. The nature of using such a outcome measure is that the analysis is inherently sensitive to the choice of components, how they are scales or normalized, and the weights assigned. The

current construction of the composite index means that it is not comparable across years, as the scaling is dependent upon the sample itself. Others have provides suggestions for remedying this issue (Greco et al. 2019), namely by fixing the scaling parameters to external information or a reference sample. For instance, any new data is scaled using the mean and standard deviation used to scale the initial sample. Alternative weighting schemes are also presented in other papers (Fernando et al. 2012), such as factor analysis.

However, the accuracy of my index for modeling the latent variable of property risk is still unknown. Validation of such an index would be possible given a small sample of high quality data, however the previously mentioned complication of accessing high quality insurance claim and loss data made that unfeasible for this study. This is a clear area of improvement that would affect our model performance and interpretation. In the absence of a validation set, more research could be done to better align our component selection and component weighting scheme with how the industry computes risk and exposure, as well as set premiums for property insurance. This, however, could be a potential study in an of itself, and thus fell outside the scope of this paper.

5 Conclusion

This paper hoped to use winter weather climate data to model underlying property risk. The use of a composite risk index instead of asset-level risk and loss data complicated the analysis, however if more research suggests sufficient alignment of our choice of components for our index with actual underlying property risk, then this paper presents a valuable initial exploration to understand the relationship between winter weather and property risk in the Great Lakes Region.

SUPPLEMENTARY MATERIAL

All code used to generate this analysis is available in the repository linked below.

Github Repository: https://github.com/acfinch-gwu/spatial-copula-winter-weather.git

References

Bacro, J.-N. & Gaetan, C. (2012), 'Max-stable processes and spatial extremes', *HAL (Le Centre pour la Communication Scientifique Directe)* .

Bureau, U. C. (n.d.), 'American Community Survey Data'. Section: Government.
URL: *https://www.census.gov/programs-surveys/acs/data.html*

Cerda, M. d. S. F., Moel, H. d., Ederen, D. v., Aerts, J., Botzen, W. J. W. & Haer, T. (2024), 'Empirical evaluation of windstorm losses and meteorological variables over the Netherlands', *Natural Hazards* .
URL: *https://doi.org/10.1007/s11069-024-07024-y*

Changnon, S. A. (2007), 'Catastrophic winter storms: An escalating problem', *Climatic Change* .
URL: *https://doi.org/10.1007/s10584-007-9289-5*

Changnon, S. A., Changnon, J. M. & Hewings, G. J. D. (2001), 'Losses caused by weather and climate extremes: A national index for the united states', *Physical Geography* .
URL: *https://doi.org/10.1080/02723646.2001.10642727*

Cohen, J., Screen, J. A., Furtado, J. C., Barlow, M., Whittleston, D., Coumou, D., Francis, J. A., Dethloff, K., Entekhabi, D., Overland, J. E. & Jones, J. (2014), 'Recent Arctic amplification and extreme mid-latitude weather', *Nature Geoscience* .
URL: *https://doi.org/10.1038/ngeo2234*

Cusack, S. (2023), 'A long record of European windstorm losses and its comparison to standard climate indices', *Natural Hazards and Earth System Sciences* .
URL: *https://doi.org/10.5194/nhess-23-2841-2023*

Earth Science Data Systems, N. (2025), 'Daymet: Daily Surface Weather Data on a 1-km Grid for North America, Version 4 R1 | NASA Earthdata'.

URL: *https://www.earthdata.nasa.gov/data/catalog/ornl-cloud-daymet-daily-v4r1-2129-4.1*

Ederen, D. v., Cerda, S., Botzen, W. J. W., Aerts, J. C. J. H., Lupi, V., Scussolini, P. & Gubbels, K. B. (2024), 'A high-resolution compound vulnerability function for European winter storm losses', *Research Square (Research Square)* .

URL: *https://doi.org/10.21203/rs.3.rs-5618142/v1*

Fernando, M., Samita, S. & Abeynayake, R. (2012), 'Modified factor analysis to construct composite indices: illustration on urbanization index.'.

URL: *https://doi.org/10.4038/TAR.V23I4.4868*

Greco, S., Ishizaka, A., Tasiou, M. & Torrisi, G. (2019), 'On the Methodological Framework of Composite Indices: A Review of the Issues of Weighting, Aggregation, and Robustness', *Social Indicators Research* .

URL: *https://doi.org/10.1007/s11205-017-1832-9*

Huser, R., Opitz, T. & Wadsworth, J. (2024), 'Modeling of spatial extremes in environmental data science: time to move away from max-stable processes'.

Klawa, M. & Ulbrich, U. (2003), 'A model for the estimation of storm losses and the identification of severe winter storms in Germany'.

URL: *https://doi.org/10.5194/NHESS-3-725-2003*

Koch, E. (2017), 'Spatial risk measures and applications to max-stable processes'.

URL: *https://doi.org/10.1007/s10687-016-0274-0*

Kug, J.-S., Jeong, J.-H., Jang, Y.-S., Kim, B.-M., Folland, C. K., Min, S.-K. & Son, S.-W. (2015), 'Two distinct influences of Arctic warming on cold winters over North America and East Asia', *Nature Geoscience* .

URL: *https://doi.org/10.1038/ngeo2517*

Mazziotta, M. & Pareto, A. (2013), 'METHODS FOR CONSTRUCTING COMPOSITE INDICES: ONE FOR ALL OR ALL FOR ONE?'.

Mazziotta, M. & Pareto, A. (2016), 'ON THE CONSTRUCTION OF COMPOSITE INDICES BY PRINCIPAL COMPONENTS ANALYSIS'.

URL: *https://econpapers.repec.org/RePEc:ite:iteeco:160103*

Moemken, J., Alifdini, I., Ramos, A. M., Georgiadis, A., Brocklehurst, A., Braun, L. & Pinto, J. G. (2024), 'Insurance loss model vs. meteorological loss index – how comparable are their loss estimates for European windstorms?', *Natural Hazards and Earth System Sciences* .

URL: *https://doi.org/10.5194/nhess-24-3445-2024*

Nardo, M., Saisana, M., Saltelli, A., Tarantola, S., Hoffman, A. N. & Giovannini, E. (2005), 'Handbook on Constructing Composite Indicators: Methodology and User Guide'.

URL: *https://doi.org/10.1787/533411815016*

Ribatet, M. (2013), 'Spatial extremes: Max-stable processes at work', *HAL (Le Centre pour la Communication Scientifique Directe)* .

URL: *https://dialnet.unirioja.es/servlet/articulo?codigo=4553863*

Schwierz, C., Köllner-Heck, P., Mutter, E. Z., Bresch, D. N., Vidale, P. L., Wild, M. & Schär, C. (2010), 'Modelling European winter wind storm losses in current and future climate', *Climatic Change* .

URL: *https://doi.org/10.1007/s10584-009-9712-1*

Segers, J. (2012), 'Max-stable models for multivariate extremes'.

URL: *https://arxiv.org/pdf/1204.0332.pdf*

Severino, L., Kropf, C. M., Afargan-Gerstman, H., Fairless, C., Vries, A. J. d., Domeisen, D. I. V. & Bresch, D. N. (2023), 'Projections and uncertainties of future winter windstorm

damage in Europe'.

URL: *https://doi.org/10.5194/egusphere-egu23-797*

Shimkus, C., Ting, M., Booth, J., Adamo, S., Madajewicz, M., Kushnir, Y. & Rieder, H. (2017), 'Winter storm intensity, hazards, and property losses in the New York tristate area', *Annals of the New York Academy of Sciences* .

URL: *https://doi.org/10.1111/nyas.13396*

Simpson, E. S., Opitz, T. & Wadsworth, J. L. (2023), 'High-dimensional modeling of spatial and spatio-temporal conditional extremes using INLA and Gaussian Markov random fields'.

URL: *https://doi.org/10.1007/s10687-023-00468-8*

Vandeskog, S. M., Martino, S. & Huser, R. (2024), 'An efficient workflow for modelling high-dimensional spatial extremes', *Statistics and computing* .

URL: *https://doi.org/10.1007/s11222-024-10448-y*

Wadsworth, J. & Tawn, J. (2012), 'Dependence modelling for spatial extremes'.

URL: *https://doi.org/10.1093/BIOMET/ASR080*

Welker, C. S., Röösli, T. & Bresch, D. N. (2021), 'Comparing an insurer's perspective on building damages with modelled damages from pan-European winter windstorm event sets: a case study from Zurich, Switzerland', *Natural Hazards and Earth System Sciences* .

URL: *https://doi.org/10.5194/nhess-21-279-2021*

Williams, R., Maycock, A. C., Charnay, V., Knight, J. & Polichtchouk, I. (2025), 'Strong polar vortex favoured intense Northern European storminess in February 2022', *Communications Earth & Environment* .

URL: *https://pubmed.ncbi.nlm.nih.gov/40161496*

6 Appendix

6.1 Appendix: Seasonal Lag Model Estimates

Table 8: Model Estimates - PCA Weighted Composite Index

Seasonal Lag Model

term	edf	ref.df	statistic	p.value
s(prcp_PC1)	7.109401	7.513508	10.799006	0.0000000
s(prcp_PC2)	4.316693	5.140227	4.797528	0.0002039
s(prcp_PC3)	6.631780	7.077755	16.996037	0.0000000
s(swe_PC1)	5.842673	6.505560	17.308488	0.0000000
s(swe_PC2)	4.117635	4.865977	4.246467	0.0031883
s(swe_PC3)	2.471157	3.091793	2.230288	0.0792512
s(tmin_PC1)	6.358335	7.041389	6.588654	0.0000000
s(tmin_PC2)	6.759961	7.162835	14.813171	0.0000000
s(tmin_PC3)	6.607557	7.071974	10.040908	0.0000000
s(tmax_PC1)	5.959436	6.700194	9.378797	0.0000000
s(tmax_PC2)	6.376529	6.889409	12.390843	0.0000000
s(tmax_PC3)	6.298740	6.849654	8.811323	0.0000000
s(prcp_PC1_lag1)	6.978861	7.379054	10.736992	0.0000000
s(prcp_PC2_lag1)	7.381923	7.827480	13.625807	0.0000000
s(prcp_PC3_lag1)	6.707521	7.131540	9.978010	0.0000000
s(swe_PC1_lag1)	4.906848	5.657684	9.185246	0.0000000
s(swe_PC2_lag1)	3.814431	4.551820	11.447421	0.0000000
s(swe_PC3_lag1)	2.587868	3.228853	2.204917	0.0953896
s(tmin_PC1_lag1)	6.901531	7.465968	26.215365	0.0000000

Continued on next page

term	edf	ref.df	statistic	p.value
s(tmin_PC2_lag1)	5.202707	6.024502	7.851354	0.0000000
s(tmin_PC3_lag1)	6.617839	7.081579	34.209291	0.0000000
s(tmax_PC1_lag1)	6.172771	6.858293	16.112076	0.0000000
s(tmax_PC2_lag1)	6.132916	6.739602	15.351372	0.0000000
s(tmax_PC3_lag1)	7.034484	7.456558	10.836216	0.0000000
s(year)	2.208298	3.000000	3.068537	0.0036452

Table 9: Model Estimates - Manually Weighted Composite Index Seasonal Lag Model

term	edf	ref.df	statistic	p.value
s(prcp_PC1)	7.011595	7.410393	13.9815222	0.0000000
s(prcp_PC2)	5.045896	5.845971	6.7446877	-0.0000005
s(prcp_PC3)	6.464434	6.970658	17.1761634	0.0000000
s(swe_PC1)	5.289695	6.006723	9.6151576	0.0000000
s(swe_PC2)	4.984092	5.673570	6.4698892	0.0000286
s(swe_PC3)	1.125077	1.231174	0.0362193	0.9344444
s(tmin_PC1)	5.921075	6.714173	7.0965167	-0.0000011
s(tmin_PC2)	6.854653	7.230882	14.5757101	0.0000000
s(tmin_PC3)	4.725746	5.582324	6.5545767	0.0000006
s(tmax_PC1)	6.571709	7.141445	17.7401764	0.0000000
s(tmax_PC2)	6.352306	6.870274	15.5526549	0.0000000
s(tmax_PC3)	6.259847	6.819047	11.4384616	0.0000000
s(prcp_PC1_lag1)	6.875012	7.282584	14.1260454	0.0000000

Continued on next page

term	edf	ref.df	statistic	p.value
s(prcp_PC2_lag1)	7.467708	7.916189	16.8774538	0.0000000
s(prcp_PC3_lag1)	6.545268	7.025703	7.6447262	0.0000000
s(swe_PC1_lag1)	3.931219	4.722881	5.8885218	0.0000481
s(swe_PC2_lag1)	2.499837	3.143056	12.9709563	0.0000000
s(swe_PC3_lag1)	2.160747	2.715593	5.1964007	0.0126160
s(tmin_PC1_lag1)	6.553135	7.170280	28.5734340	0.0000000
s(tmin_PC2_lag1)	2.648558	3.404820	9.9945495	0.0000008
s(tmin_PC3_lag1)	6.572912	7.044292	37.7280706	0.0000000
s(tmax_PC1_lag1)	4.821099	5.793793	16.5629836	0.0000000
s(tmax_PC2_lag1)	5.960346	6.612793	13.3681628	0.0000000
s(tmax_PC3_lag1)	7.331748	7.780325	17.0336404	0.0000000
s(year)	1.967876	3.000000	1.9127491	0.0215894